Reduced Order Models for Metamaterial Transmission Lines

Giulio Antonini, *Senior Member*, *IEEE*
UAq EMC Laboratory
Dipartimento di Ingegneria Elettrica e dell'Informazione
Università degli Studi di L'Aquila
Monteluco di Roio, 67040 AQ, Italy

Abstract - **This paper presents a reduced order model of metamaterial transmission lines. The metamaterial transmission line can be regarded as a ladder network characterized by propagating and evanescent modes generated by negative permeability and permittivity. Quasi-closed form of poles and residues are computed, taking advantage of the periodic structure of such type of structure, thus leading to an efficient time domain macromodel. Furthermore, the same methodology can be also efficiently used when the metamaterial is characterized in terms of equivalent dispersive and lossy permeability and permittivity over a frequency range. A model order reduction (MOR) technique is proposed allowing to reduce the computational effort in carrying out time domain simulations and allowing fast parametric models generation. In addition, the capability of the proposed method to properly reproduce the physics of metamaterials and to reduce the computational complexity due to the dispersive behavior of such artificial materials is demonstrated by the numerical results.**

Index terms-**Metamaterials, transient analysis, dispersive and lossy materials, model-order reduction techniques, parametric models.**

I. Introduction

In the late 1960s, Veselago proposed that materials with simultaneously negative permittivity and permeability are physically permissible and have a negative index of rifraction [1], [2]. He called these left-handed (LH) materials because the vectors $\boldsymbol{E}$, $\boldsymbol{H}$ and $\boldsymbol{k}$ form a left-handed triplet instead of right-handed triplet, as in the case of conventional right-handed (RH) media. Although it has been known for some time that arrays of thin metallic wires can produce an effectively negative dielectric permittivity, it was not clear as to how produce a negative permeability until the recent development of the split-ring resonator (SRR) by Pendry *et al.* was successful in this effort [3]. Experimental evidence of LH materials properties has been given by Smith *et al.* [4], [5] who demonstrated an LH structure made of negative-ε thin-wires and negative-μ split-ring resonators exhibiting anomalous refraction at the boundary. More than 30 years passed before such media, referred to as *metamaterials* (MTMs), were first realized by several research groups [4]-[7], based on resonant periodic structures with series capacitors and shunt inductors.

Such artificial media are characterized by negative values of permeability and permittivity over a wide frequency band and exhibit an evident and necessary dispersive behavior [2] which requires a special care when implementing a time domain algorithm. So far metamaterials have been extensively studied in the frequency domain and only recently time domain schemes have been proposed to capture the dispersive nature of the metamaterial itself. In [8] a one-dimensional (1-D) Finite Difference Time Domain (FDTD) method is presented to investigate the super-luminal properties of a particular type of metamaterial, the two time derivative Lorentz material (2TDLM), in propagating signals through the medium. Although the obtained results allow to gain deeper insight into the physics of such materials, the developed FDTD code is complex to be implemented and simulations are quite time-memory consuming. Also in [9] the behavior of an evanescent wave interacting with a slab of a backward material with Lorentz-type frequency dependence is studied via FDTD simulations based on a pseudo-spectral time domain (PSTD) method [10]. As in the previous work, a dedicated algorithm

Corresponding Author: G. Antonini, *UAq EMC Laboratory*, Dipartimento di Ingegneria Elettrica, Università degli Studi di L'Aquila, Monteluco di Roio, 67040, L'Aquila, Italy. Tel.:+39-0862-434462, fax: +39-0862-434403, e-mail: antonini@ing.univaq.it

must be implemented to perform time domain computations and a special care is required to ensure the necessary stability.

One of the most successful approaches to model left-handed (LH) materials has been presented in [7] where an equivalent circuit for a left-handed transmission line (LH-TL) is proposed. Such equivalent circuit has been then extended to composite right/left handed (CRLH) metamaterials in [11]. A more complex unit cell of the equivalent line circuit of a metamaterial constituted by a split-ring resonator/wire medium is presented in [6]. The same authors have presented in [12] a two-dimensional (2-D) L, C loaded transmission line acting as an isotropic left handed or negative refracting index (NRI) material. In [13] a 2-D Composite right/left handed transmission line (CRLH-TL) model is presented and the dispersion diagram of the two-dimensional CRLH-TL is obtained analytically based on the Bloch-Floquet theory. The main advantage of a circuit description is that the same equivalent circuit can be used in both the frequency and time domain computations; the main drawback is that the proposed circuits assume particular dispersive laws of the material and cannot be used to model different type of metamaterials (e.g. 2TDLM).

One of the most challenging task in using metamaterials in practical applications is their miniaturization in order to make them well suited for mobile communication systems. Much progress has been recently done as shown in [14] where a super-compact diplexer is presented and characterized as a multilayered composite left/right transmission line (ML-CRLH-TL).

Metamaterials surely will keep drawing interest in the microwave community and new artificial materials belonging to their family will be designed and new devices will be constructed. This increasing interest in MTMs calls for new numerical techniques which are able to reproduce their intrinsic dispersive nature at a reduced cost. Nowadays, as pointed out above, time domain methods require a special care, when dealing with dispersive media, which causes them to be extremely more time consuming when compared with their non-dispersive counterpart.

More recently time domain modeling of MTMs has received an increasing interest and led to the publication of several papers on it [15]-[17] where 2D and 3D numerical models are presented. As several practical implementations of MTMs are based on circuit and transmission lines, one of the most used techniques for modeling such kind of materials is the Transmission Line Matrix (TLM) method [18], [19].

Aim of this work is to present a novel methodology for the transient analysis of metamaterial transmission lines (MMTLs) exhibiting a general dispersive behavior, based on the analytical characterization of the half-T ladder network approximating the metamaterial transmission line. The most important features of the proposed approach are: 1) it allows straightforward computation of the poles of the two-port representation of the MMTL with machine-accuracy; 2) the knowledge of the MMTL poles allows to generate a macromodel which can be used in both time and frequency domain; 3) the knowledge of the poles allows developing a reduced order model, by retaining only the poles which significantly impact the physical behavior of the MMTL in the frequency range of interest; 4) the proposed method can be used for any type of metamaterial as it doesn't assume any particular kind of dispersive behavior nor law for negative equivalent parameters μ and ε; 5) the proposed methodology can be used as building block for modeling metamaterials and, in general, dispersive media, in the framework of the TLM method [19]-[16]; 6) a quasi analytical correspondence between per-unit length parameters of the MMTL and the poles of the system is extremely useful at the design stage as it allows to select the stop and pass-bands and, thus, to design the frequency response of the system; 7) parameterized reduced order models can be easily generated.

The paper is organized as follows. Section II presents the formulation for modeling MMTLs with general constitutive parameters of equivalent materials. In Section III the two port representation of the MMTL in both the cases of CRLH and 2DTLM metamaterials is presented; in Section IV relevant formulas for computing poles and residues of CRLH materials are derived. The knowledge of poles allows to select only the dominant ones, within a fixed frequency band, that really impact the physical

behavior of the MMTL; the pole pruning is described in Section V pointing out that a special care is needed in order to ensure high accuracy as the interaction of longitudinal and transversal resonators cause the poles to be located mostly in well separated frequency bands. The possibility to adopt the proposed method to generate parameterized macromodels of MMTL is reported in Section VI. Numerical results for CRLH and 2DTLM MMTLs are presented in Section VII where the accuracy of the proposed method in reproducing the physical behavior of MMTLs is demonstrated along with the reduction of the computational complexity. Section VIII draws the conclusions.

II. General formulation for propagating and evanescent modes

Several previous studies of metamaterials have been carried out considering the propagation of electromagnetic signals through a slab characterized by negative ε and μ over a frequency range [8]; more recently a composite right/left handed transmission line has been presented [7], [11] and studied by using standard techniques in the frequency domain. Both these two problems can be studied by means of the transmission line theory (TLT). Thus, we will start by considering the first kind of problem keeping in mind that the second one can be analyzed by using the same formalism. Fig. 1 shows an uniform plane wave normally impinging on a slab of a metamaterial.

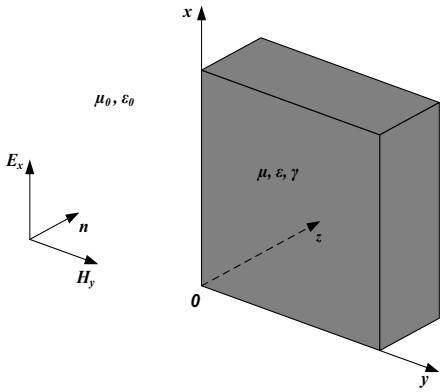

Fig. 1. An uniform TEM plane wave impinging on a slab of metamaterial.

Although the methodology illustrated in the following holds also for non orthogonal incidence [22], for the sake of clarity, only the orthogonal incidence will be here presented. For a $\boldsymbol{E}_x - \boldsymbol{H}_y$ TEM uniform plane wave Maxwell's equations in Laplace's domain read:

$$\frac{\partial}{\partial z}\boldsymbol{E}_x(z,s) = -s\mu(s)\,\boldsymbol{H}_y(z,s) \tag{1a}$$

$$\frac{\partial}{\partial z}\boldsymbol{H}_y(z,s) = -(s\varepsilon(s)+\gamma)\,\boldsymbol{E}_x(z,s) \tag{1b}$$

where $\mu(s)$ and $\varepsilon(s)$ are the frequency dependent permeability and permittivity of the metamaterial and γ its electric conductivity. The difficulty in finding the transient solution of such kind of equations is related to the dispersive behavior of the $\mu(s)$ and $\varepsilon(s)$ parameters which requires a special treatment. The physics of metamaterials is strictly related to the fact that they exhibit simultaneously negative permeability and permittivity. As pointed out before, TEM propagation through a slab can be studied by using transmission line theory (TLT). In the case of metamaterials the per unit length parameters of the equivalent transmission line may be frequency dependent making their transient analysis an even more difficult task.

The development of transient analysis algorithms for lossy and dispersive transmission lines with frequency dependent parameters has recently received much attention and efficient techniques have

been proposed [23]-[27]. In these papers MOR techniques, based on Padé approximations, together with the state-space formulation of the solution of the transmission line system, are used to develop reduced-order macromodels of the transmission line (TL). More recently a new method has been presented [28] based on half-T ladder network (HTLN) theory and special polynomials known as DFF and DDFz [29]-[31], allows the extraction of poles and residues of the half-T ladder network approximating the MTL which pawns the way to an efficient model order reduction technique; the method has been more recently extended to frequency dependent per unit length parameters (FDPUL) [32] and will be rapidly reviewed in Section III. Although the methodology illustrated in [32] can be adopted *tout-court* to capture the physics of CRLH metamaterials which exhibit a dispersive behavior along with their typical properties such as backward waves [33], a different approach is used in this work. An HTLN is considered to model both the metamaterial slab or transmission line. Thus, in the following, we will refer indifferently to the slab and the transmission line.

A classification of metamaterials can be done according to the kind of dispersion from which they are characterized. We will consider two classes of metamaterials which are widely studied in the literature and used for practical applications: CRLH and 2TDLM metamaterials.

A. CRLH metamaterials

Such kind of artificial materials have a simple equivalent circuit synthesis. In [34] the authors show that both propagating and evanescent TM modes exist in double negative media (DNG) and equivalent TL models have been proposed which are characterized by longitudinal capacitances and transversal inductances. The same typology of elementary halt-T cell is adopted in [11]. For this reason in the following it will be assumed the equivalent circuit shown in Fig. 2 which represents a possible model for an electrically short section of a composite right/left handed transmission line (CRLH-TL), although more complex models can be considered; sub-indexes R and L refer to right and left handed properties.

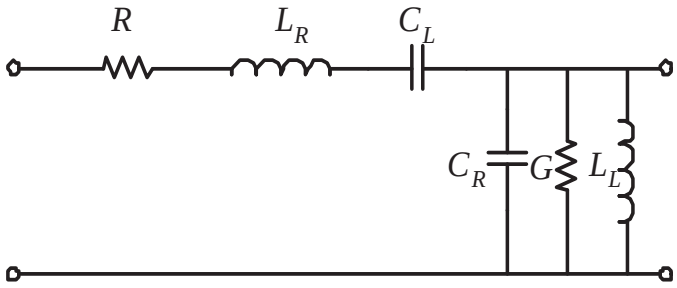

Fig. 2. Elementary half-T cell for a CRLH-TL.

Transient analysis of TLs, under the assumption that only the TEM mode propagates, is based on the set of partial differential equations known as Telegrapher's equations which, in Laplace domain, are given by:

$$\frac{\partial}{\partial z}V(z,s) = -\left(R' + sL'_R + \frac{1}{s}C'^{-1}_L\right) I(z,s) \tag{2a}$$

$$\frac{\partial}{\partial z}I(z,s) = -\left(G' + sC'_R + \frac{1}{s}L'^{-1}_L\right) V(z,s) \tag{2b}$$

where $R' \in \Re$, $L'_R \in \Re$, $C'_R \in \Re$, $G' \in \Re$, $L'_L \in \Re$ and $C'_L \in \Re$ are frequency-independent per-unit-length (FIPUL) parameters [35], [36]. The exponential form of Telegrapher's equations [35], in the

case of FIPUL parameters, reads:

$$\begin{bmatrix} V(\ell,s) \\ -I(\ell,s) \end{bmatrix} = e^{\Psi} \begin{bmatrix} V(0,s) \\ I(0,s) \end{bmatrix} \tag{3}$$

where

$$\Psi(s) = \left(\alpha + s\beta + \frac{1}{s}\gamma\right)\ell \qquad \alpha = \begin{bmatrix} 0 & -R' \\ -G' & 0 \end{bmatrix} \qquad \beta = \begin{bmatrix} 0 & -L'_R \\ -C'_R & 0 \end{bmatrix} \quad \gamma = \begin{bmatrix} 0 & -C'^{-1}_L \\ -L'^{-1}_L & 0 \end{bmatrix} \tag{4}$$

It is easy to verify that the equivalent circuit described in Fig. 2 is adeguate to model the basic property of CRLH media which is the simultaneous negativity, at least within a certain frequency range, of permittivity and permeability. This is essential to correctly model such as backward waves and evanescent modes. For a lossless material the propagation constant is $\beta = \omega\sqrt{\mu\varepsilon}$; thus, as the propagation constant of a TL is $j\beta = \sqrt{Z'Y'}$, the following relation can be set up [11]:

$$-\omega^2\mu\varepsilon = Z'Y' \tag{5}$$

Furthermore, the TL's characteristic impedance $Z_c = \sqrt{Z'/Y'}$ and the material's intrinsic impedance $\eta = \sqrt{\mu/\varepsilon}$ can be related such that

$$Z_c = \eta \rightarrow \frac{Z'}{Y'} = \frac{\mu}{\varepsilon} \tag{6}$$

Finally, equivalent magnetic permeability and electric permittivity can be written as

$$\mu(\omega) = \frac{Z'}{j\omega} = L'_R - \frac{1}{\omega^2 C'_L} \tag{7}$$

$$\varepsilon(\omega) = \frac{Y'}{j\omega} = C'_R - \frac{1}{\omega^2 L'_L} \tag{8}$$

which can be negative up to a given frequency determined by the values of per unit length right and left parameters. The corresponding parameters in the Laplace domain read:

$$\mu(s) = \frac{Z'}{s} = L'_R + \frac{1}{s^2 C'_L} \tag{9}$$

$$\varepsilon(s) = \frac{Y'}{s} = C'_R + \frac{1}{s^2 L'_L} \tag{10}$$

B. 2DTLM medium

In [8] it has been presented a different metamaterial model, the two time derivative Lorentz material (2TDLM), which can be designed so that it allows communication signals to propagate in the medium at speeds exceeding the speed of light in vacuum without violating causality. Such a medium is characterized by frequency dependent parameters μ and ε:

$$\mu(s) = \mu_0\left[1 + \chi^m_{2TDLM}(s)\right] \tag{11}$$

$$\varepsilon(s) = \varepsilon_0\left[1 + \chi^e_{2TDLM}(s)\right] \tag{12}$$

where the Laplace domain electric and magnetic susceptibilities $\chi_{2TDLM}(s)$ are:

$$\chi^m_{2TDLM}(s) = \chi^e_{2TDLM}(s) = \chi_{2TDLM}(s) = \frac{\omega_p^2\chi_\alpha + s\omega_p\chi_\beta + s^2\chi_\gamma}{s^2 + s\Gamma + \omega_0^2} \tag{13}$$

This choice of the parameters guarantees that the wave impedance in this matched 2DTLM medium equals that from the free space thus leading to a zero reflection coefficient. Properly setting the parameters in (13) leads to values of μ and ε smaller than their values in free space over a large range of frequencies.

The previous model for μ and ε can be easily synthesized into equivalent circuits which look like with those in Fig. 2. In the case of more complex dispersive behaviors (e.g. when higher order rational representations are used for $\chi_{2TDLM}(s)$) it is always possible to use the HTLN model; in fact, an equivalent HTLN can be built to model such a medium which is characterized by frequency dependent per unit length parameters. In this case Telegrapher's equations, in Laplace domain, are given by:

$$\frac{\partial}{\partial z}V(z,s) = -\left(R'(s)+sL'(s)\right)I(z,s) \tag{14a}$$

$$\frac{\partial}{\partial z}I(z,s) = -\left(G'(s)+sC'(s)\right)V(z,s) \tag{14b}$$

where $R'(s) \in \Re$, $L'(s) \in \Re$, $C'(s) \in \Re$, $G'(s) \in \Re$ are frequency-dependent per-unit-length (FD-PUL) parameters. Equations (14a-14b) can be re-written in the Laplace domain by using the same exponential matrix function as in (3) where, in this case, Ψ reads

$$\Psi(s) = \left(\alpha(s)+s\beta(s)\right)l \qquad \alpha = \begin{bmatrix} 0 & -R'(s) \\ -G'(s) & 0 \end{bmatrix} \qquad \beta(s) = \begin{bmatrix} 0 & -L'(s) \\ -C'(s) & 0 \end{bmatrix} \tag{15}$$

III. Two port representation

A. FIPUL parameters

Let's assume that an order n half-T ladder network (HTLN) is used for approximating the TEM modes in the metamaterial slab or MMTL; the parameters for a single cell are:

$$R = R'\frac{\ell}{n} \qquad L_R = L'_R\frac{\ell}{n} \qquad C_L = C'_L\frac{n}{\ell} \tag{16a}$$

$$G = G'\frac{\ell}{n} \qquad C_R = C'_R\frac{\ell}{n} \qquad L_L = L'_L\frac{n}{\ell} \tag{16b}$$

where ℓ is the thickness of the slab or the length of the transmission line. The unit cell quantities can be defined as:

$$Z_1(s) = \left(R'+sL'_R+\frac{1}{sC'_L}\right)\frac{\ell}{n} = Z'(s)\frac{\ell}{n} = R+sL_R+\frac{1}{sC_L} \tag{17a}$$

$$Y_2(s) = \left(G'+sC'_R+\frac{1}{sL'_L}\right)\frac{\ell}{n} = Y'(s)\frac{\ell}{n} = G+sC_R+\frac{1}{sL_L} \tag{17b}$$

The standard case of RH propagation presented in [28],[32] is obtained when $L_L = C_L = \infty$.

B. FDPUL parameters

In the case of FDPUL parameters it is assumed that a suitable rational approximation of $Z_1(s)$ and $Y_2(s)$ matrices is obtained by using standard fitting techniques [37], leading to the following rational representations:

$$Z_1(s) \cong Z_{fit,1}(s) = R_0 + sL_0 + \sum_{m=1}^{P_1}\frac{R_1}{s-p_{m,1}} \tag{18a}$$

$$Y_2(s) \cong Y_{fit,2}(s) = G_0 + sC_0 + \sum_{m=1}^{P_2}\frac{R_2}{s-p_{m,2}} \tag{18b}$$

where P_1 and P_2 represent the number of poles used in the rational approximation.
The zero-pole form is better suited for algebraic manipulations and polynomials convolutions [38]; for matrices Z_1 and Y_2 it reads:

$$Z_1(s) \cong \frac{b_1 s^{P_1+1} + b_2 s^{P_1} s + \cdots + b_{P_1} s + b_{P_1+1}}{a_1 s^{P_1} + a_2 s^{P_1-1} + \cdots + a_{P_1} s + a_{P_1+1}} = \frac{B_p(s)}{A_p(s)} \tag{19a}$$

$$Y_2(s) \cong \frac{d_1 s^{P_2+1} + d_2 s^{P_2} s + \cdots + d_{P_2} s + d_{P_2+1}}{c_1 s^{P_2} + c_2 s^{P_2-1} + \cdots + c_{P_2} s + c_{P_2+1}} = \frac{D_p(s)}{C_p(s)} \tag{19b}$$

where $B_p(s)$ and $D_p(s)$ are positive real polynomial and $A_p(s)$ and $C_p(s)$ are strictly Hurwitz polynomials. A strict Hurwitz polynomial has its roots only in the left half-plane. Hence, the poles of the rational approximations (19) are strictly in the left half-plane.

C. Y matrix representation

In [30] it has been shown that a half-T ladder network can be analytically characterized in terms of Chebyshev polynomials. The polynomial based approach presented in [30] and then extended to transmission lines in [28],[32],[39] is here briefly summarized for the sake of clarity. To this aim let's define the half-T cell factor $K(s)$ as:

$$K(s) = Z_1(s)\, Y_2(s) \tag{20}$$

In [30] it was shown that all the electrical characteristics of a HTLN can be expressed in terms of two polynomials (namely DFF and DFFz) depending on the cell matrix factor $K(s)$:

$$P_b^n(K(s)) = \sum_{j=0}^{n} b_{j,n} K^j(s) \qquad \text{DFF polynomial of order } n \tag{21}$$

$$P_c^n(K(s)) = \sum_{j=0}^{n} c_{j,n} K^{j+1}(s) \qquad \text{DFFz polynomial of order } n \tag{22}$$

where coefficients $b_{j,n}$ and $c_{j,n}$ can be computed analytically as:

$$b_{i,j} = \begin{pmatrix} i+j \\ j-i \end{pmatrix} \tag{23a}$$

$$c_{i,j} = \begin{pmatrix} i+j+1 \\ j-i \end{pmatrix} \tag{23b}$$

Two port A, B, C and D parameters can be expressed in terms of DFF and DFFz polynomials as:

$$\mathrm{A}(s) = \sum_{j=0}^{n} b_{j,n} K^j(s) = P_b^n(K(s)) \tag{24a}$$

$$\mathrm{B}(s) = \left(\sum_{j=0}^{n} c_{j,n} K^{j+1}(s) \right) \cdot Y_2^{-1}(s) = P_c^n(K(s)) \cdot Y_2^{-1}(s) \tag{24b}$$

$$\mathrm{C}(s) = Z_1^{-1}(s) \cdot \left(\sum_{j=0}^{n} c_{j,n} K^{j+1}(s) \right) = Z_1^{-1}(s) \cdot P_c^n(K(s)) \tag{24c}$$

$$\mathrm{D}(s) = \sum_{j=0}^{n-1} b_{j,n-1} K^j(s)^T = P_b^{n-1}(K(s))^T \tag{24d}$$

The knowledge of the ABCD representation allows to obtain any two port matrix representation. In the case of linear and isotropic media the symmetry and reciprocity properties hold thus ensuring that $\mathrm{D} = \mathrm{A}^T$, $\mathrm{B} = \mathrm{B}^T$, $\mathrm{C} = \mathrm{C}^T$ and that $det\,(\mathrm{AD} - \mathrm{BC}) = 1$.

The Y matrix entries can be evaluated by computing Y_{11} and Y_{21} in terms of ABCD parameters and then by enforcing the reciprocity and symmetry of the transmission line.

$$Y_{11} = \mathrm{DB}^{-1} = P_b^{n-1}\left(K(s)\right) \cdot \left(P_c^n\left(K(s)\right) \cdot Y_2^{-1}(s)\right)^{-1} \tag{25a}$$

$$Y_{21} = -\mathrm{B}^{-1} = -\left(P_c^n\left(K(s)\right) \cdot Y_2^{-1}(s)\right)^{-1} \tag{25b}$$

Reciprocity and symmetry properties of the transmission line are guaranteed by the conditions:

$$Y_{12} = Y_{21} \tag{26a}$$

$$Y_{22} = Y_{11} \tag{26b}$$

Polynomials $P_b^{n-1}\left(K(s)\right)$ and $P_c^n\left(K(s)\right)$ can be factored by using the roots presented in [28]:

$$P_b^{n-1}\left(K(s)\right) = \prod_{j=1}^{n-1}\left(K(s) - u_{j,n-1}U\right) \tag{27a}$$

$$P_c^n\left(K(s)\right) = \prod_{j=1}^{n-1}\left(K(s) - v_{j,n-1}U\right) \cdot K \tag{27b}$$

where U is the unitary matrix. Considering that $K(s) \cdot Y_2^{-1}(s) = Z_1\left(s\right)$, the previous expressions (25a) and (25b) can be factored as:

$$Y_{11} = Y_{22} = \prod_{j=1}^{n-1}\left(K\left(s\right) - u_{j,n-1}U\right) \cdot \left[\prod_{j=1}^{n-1}\left(K\left(s\right) - v_{j,n-1}U\right) \cdot Z_1\left(s\right)\right]^{-1} \tag{28a}$$

$$Y_{21} = Y_{12} = -\left[\prod_{j=1}^{n-1}\left(K\left(s\right) - v_{j,n-1}U\right) \cdot Z_1\left(s\right)\right]^{-1} \tag{28b}$$

where roots $u_{j,n-1}$ and $v_{j,n-1}$ are given by [29]:

$$u_{j,n-1} = -4sin^2\left(\frac{(2j-1)}{(2n-1)}\frac{\pi}{2}\right) \qquad j = 1 \cdots n-1 \tag{29a}$$

$$v_{j,n-1} = -4sin^2\left(\frac{j\pi}{2n}\right) \qquad j = 1 \cdots n-1 \tag{29b}$$

It is to be pointed out that the frequency dependence of per unit length parameters is completely described by $K(s)$ function and that the roots $u_{j,n-1}$ and $v_{j,n-1}$ of P_b^{n-1} and P_c^n polynomials are frequency independent [30].

IV. Computation of poles and residues of MMTLs

The computation of poles and corresponding residues of transmission lines with frequency dependent per-unit length parameters requires solving the following equation:

$$\left[\prod_{j=1}^{n-1}\left(K\left(s\right) - v_{j,n-1}\right) \cdot Z_1\left(s\right)\right] = 0 \tag{30}$$

In the following we will focus on CRLH-TLs which are characterized by frequency independent parameters although their nature is complicated by the presence of left-handed parameters (C'_L and L'_L) which causes many poles to be located close to zero. The derivation leads to low order algebraic equations and allows exploiting important properties of CRLH-TLs.

A. Approximate poles of CRLH MMTLs

Poles of Y matrix functions are obtained as the zeros of the following equation:

$$\left[\prod_{j=1}^{n-1}\left(K\left(s\right)-v_{j,n-1}\right)\cdot Z_1\left(s\right)\right]=0 \tag{31}$$

thus allowing to solve n equations separately.

The poles of the HTLN can be identified as:
1. zeros of polynomial $Z_1\left(s\right)$
2. zeros of polynomial $Z_1\left(s\right)Y_2\left(s\right)-v_{j,n-1}, \qquad \text{for } j=1\cdots n-1$

A.1 Poles 1

Poles of the first type satisfy the equation:

$$s^2L_RC_L+sC_LR+1=0 \tag{32}$$

A.2 Poles 2

Poles of the second type are obtained as the solutions of the equation:

$$Z_1\left(s\right)Y_2\left(s\right)-v_{j,n-1}=0, \quad \text{for } j=1\cdots n-1 \tag{33}$$

It can be re-written in terms of parameters of the elementary CRLH cell as:

$$\left(RG+\frac{L_R}{L_L}+\frac{C_R}{C_L}\right)+s\left(RC_R+GL_R\right)+s^2L_RC_R+\frac{1}{s}\left(\frac{R}{C_L}+\frac{G}{C_L}\right)+\frac{1}{s^2}\frac{1}{L_LC_L}-v_{j,n-1}=0, \quad \text{for } j=1\cdots n-1 \tag{34}$$

In the general case, for each root $v_{j,n-1}$, the following equation is to be solved:

$$a+bs+cs^2+\frac{d}{s}+\frac{e}{s^2}=0 \tag{35}$$

where

$$a = RG+\frac{L_R}{L_L}+\frac{C_R}{C_L}-v_{j,n-1} \tag{36a}$$
$$b = RC_R+GL_R \tag{36b}$$
$$c = L_RC_R \tag{36c}$$
$$d = \frac{R}{C_L}+\frac{G}{C_L} \tag{36d}$$
$$e = \frac{1}{L_LC_L} \tag{36e}$$

The roots finally satisfy the equation

$$as^2+bs^3+cs^4+ds+e=0 \tag{37}$$

Thus, for each root $v_{j,n-1}, j=1\cdots n-1$, four different poles are generated in the CRLH case, while in the RH case only two poles corresponds to each root $v_{j,n-1}$ [39]. It is also worth considering the lossless case $R=G=0$. Coefficients b and d in (36) are zero and the equation to be solved reduces to

$$as^2+cs^4+e=0 \tag{38}$$

whose roots come in pair. As the poles of the HTLN can be computed by solving low order algebraic equations, they are continuously depending on the physical parameters (circuit parameters, length of the MMTL). This allows to claim that parameterized reduced order models corresponding to a variation of such parameters with respect to a fixed point of the parameter space can be generated just by perturbing the model for that point.

B. Computation of residues of Y matrix

Residues of pole p_i can be obtained as:

$$\begin{aligned} R_{11,i} = R_{22,i} &= \left[\left(\prod_{j=1}^{n-1}\left(K\left(s\right)-v_{j,n-1}U\right)\right)\cdot Z_1\left(s\right)\right]/ \\ &/ \quad det\left[\left(\prod_{j=1}^{n-1}\left(K\left(s\right)-v_{j,n-1}U\right)\right)\cdot Z_1\left(s\right)\right]\cdot\prod_{j=1}^{n-1}\left(K\left(s\right)-u_{j,n-1}U\right)\left(s-p_i\right)|_{s=p_i} \quad (39) \\ R_{12,i} = R_{21,i} &= -\left[\left(\prod_{j=1}^{n-1}\left(K\left(s\right)-v_{j,n-1}U\right)\right)\cdot Z_1\left(s\right)\right]/ \\ &/ \quad det\left[\left(\prod_{j=1}^{n-1}\left(K\left(s\right)-v_{j,n-1}U\right)\right)\cdot Z_1\left(s\right)\right]\cdot\left(s-p_i\right)|_{s=p_i} \quad (40) \end{aligned}$$

for $i = 1 \cdots P_Y$, being P_Y the total number of poles of the $\boldsymbol{Y}$ matrix entries.

V. Model Order Reduction

In Section III it has been shown that the proposed approach allows to provide a rational approximation of Y matrix entries (25) in terms of residues and poles whose computation is straightforward. The development of a MOR technique requires the determination of the dominant poles of the system, which significantly influence the time as well as the frequency characteristics of the system under analysis [23]. In the recent past moment-matching techniques have been widely adopted to extract the dominant poles of a given system [40]-[43]. It is known that such techniques are extremely time consuming as they require computing and matching moments; on the contrary the proposed method is extremely fast in extracting the poles among which the dominant ones have to be selected.

In [32] it has been presented a model order reduction approach which is based on a two step process: 1) poles within a given bandwidth $k\omega_{max}$ (where $k > 1$ and ω_{max} corresponds to the required bandwidth (e.g. the angular frequency beyond which the power of the excitation is negligible) are selected; 2) as the corresponding residues are known, only those that significantly impact the frequency and time responses are retained.

When dealing with metamaterials the co-existence of both longitudinal and transversal resonators (see Fig. 2) cause many poles to be located near zero; the magnitude of the corresponding residues is ordinarily small if compared to those of other poles; nevertheless they are important to correctly model the physical behavior in the low frequency range. Furthermore, it has been observed that poles are not spread over the entire frequency axis but tend to be concentrated in bandwidths which may be also far away one from each other. This fact causes the typical pass-band and stop band behavior of metamaterials frequency response. This suggests to adopt a frequency hopping poles selection within each bandwidth.

The procedure can be formalized by the following algorithm:

- the maximum angular frequency $\omega_{MOR} = k\omega_{max}$ is selected;
- the bandwidth $[-\omega_{MOR}, \omega_{MOR}]$ is subdivided in sub-bands according to a suitable algorithm;
- dominant poles selection is performed within each band.

Once the dominant poles have been selected and the corresponding residues computed, a macromodel can be generated [28] by using standard techniques.

A. Macromodel synthesis

Once the reduced order poles-residues representation of functions Y_{11}, Y_{12}, Y_{21} and Y_{22} is obtained a macromodel can be easily derived by generating the $\mathcal{ABCD}$ state-space domain representation leading to a set of first order differential equations which reads:

$$\begin{aligned} \frac{d}{dt}\mathbf{x}(\mathbf{t}) &= \mathcal{A}\mathbf{x}(\mathbf{t}) + \mathcal{B}\mathbf{u}(\mathbf{t}) \\ \mathbf{y}(\mathbf{t}) &= \mathcal{C}\mathbf{x}(\mathbf{t}) + \mathcal{D}\mathbf{u}(\mathbf{t}) \end{aligned} \tag{41}$$

where $\mathcal{A} \in \mathrm{R}^{p\times p}$, $\mathcal{B} \in \mathrm{R}^{p\times n}$, $\mathcal{C} \in \mathrm{R}^{n\times p}$, $\mathcal{D} \in \mathrm{R}^{n\times n}$, p is the number of states and n the order of the proposed model. Obviously, as the admittance matrix representation is used, the input vector $\mathbf{u}(\mathbf{t})$ and output vector $\mathbf{y}(\mathbf{t})$ correspond to port voltages $\boldsymbol{v}(t)$ or electric fields $\boldsymbol{E}_x(t)$ and currents $\boldsymbol{i}(t)$ or magnetic fields $\boldsymbol{H}_y(t)$, respectively. Since a model reduction has already been applied, a standard minimal-order realization can be efficiently used [44]-[47]. The set of first order differential equations (41) are completed with the terminal conditions and solved numerically.

VI. Parameterized macromodels for MMTLs

The design of systems and devices based on MMTLs usually requires optimization procedures which call for a fast evaluation of MMTLs performances for varying physical and geometrical parameters. The proposed method is well suited to this aim. In fact it allows an easy computation of poles and residues of the MMTLs by solving low order algebraic equations.

Let's assume that the MMTL depends on a set of physical and/or geometrical parameters $\lambda_1, \lambda_2, \cdots, \lambda_n$. Telegrapher's equations, in the case of CRLH MMTL, can be expressed as

$$\frac{\partial}{\partial z}V(z,s;\lambda) = -\left(R'(s;\lambda) + sL'_R(s;\lambda) + \frac{1}{s}C'_L(s;\lambda)^{-1}\right) I(z,s;\lambda) \tag{42a}$$

$$\frac{\partial}{\partial z}I(z,s;\lambda) = -\left(G'(s;\lambda) + sC'_R(s;\lambda) + \frac{1}{s}L'_L(s;\lambda)^{-1}\right) V(z,s;\lambda) \tag{42b}$$

The possibility to compute poles and residues of the $\boldsymbol{Y}$ matrix by solving low order algebraic equations and to select only the dominant ones is exploited for the automatic generation of reduced order parameterized models. The half-T cell factor becomes:

$$K(s;\lambda) = Z_1(s;\lambda)\, Y_2(s;\lambda) \tag{43}$$

The poles of the parameterized $\boldsymbol{Y}$ matrix functions are obtained as the zeros of the following equation:

$$\left[\prod_{j=1}^{n-1}\left(K(s;\lambda) - v_{j,n-1}\right)\cdot Z_1(s;\lambda)\right] = 0 \tag{44}$$

which implies that, as pointed before, separate algebraic equations have to be solved. As described in Section V only the dominant poles are retained to generate the reduced order model. Usually, per unit length parameters are smooth functions of geometrical parameters. As a consequence, also the solutions of (43) changes continuously with respect to the parameters. Location of dominant poles in the complex plane can be monitored at the design stage such that special performances of the MMTL can be obtained. It is worth mentioning that the ease computation of poles by solving low order algebraic equations makes this procedure to be preferred to any interpolation scheme to recover poles from unit-cell parameters. The generation of the macromodel corresponding to a generic set of unit-cell parameters in the parameter space requires the efficient computation of residues; it can be done by means of (39) or, as an alternative, by multidimensional linear interpolation.

VII. Numerical results

A. Unbalanced CRLH-TL

As a first example it has been considered the lossless CRLH-TL described in [11], with global parameters $R = 10^{-3}\ \Omega, L_R = 2.45$ nH, $C_L = 0.68$ pF, $G = 10^{-3}$ S, $C_R = 0.5$ pF and $L_L = 3.38$ nH and a length $l = 6.1$ mm. Fig. 3 shows the dispersion diagram for such material along with the linear dispersive curve and that of the balanced case ($L_R C_L = L_L C_R$).

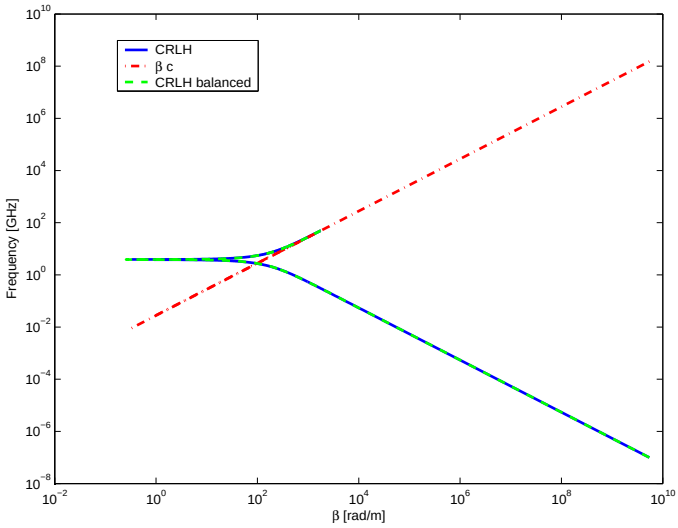

Fig. 3. Dispersion diagram for the CRLH-TL of example VII-A.

The effective permeability and permittivity (7) have been computed exhibiting simultaneous negative values up to about 4 GHz; their magnitude is shown in Fig. 4.

The ABCD parameters have been computed in the frequency range 0-50 GHz by using the transmission line theory (TLT), the half-T ladder network (HTLN) and the polynomial representation (DFF). Fig. 5 shows the comparison of coefficients A, B, C and D as evaluated by the three techniques. As clearly seen the results are in a good agreement over the entire frequency range. As pointed out in Section V, the higher complexity of the unit cell of CRLH-TLs, with respect to the one of standard RH-TLs, causes the low frequency behavior to be much more complex, thus requiring great attention in applying the model order reduction.

Fig. 6 shows the poles of the $\boldsymbol{Y}$ matrix entries in the complex plane. As seen, all the poles lie in the left-half complex plane thus strictly ensuring the stability of the model.

The co-existence of two resonators in the unit cell makes the low frequency and high frequency behaviors not well separated in the sense that there are low frequencies resonances (below 200 MHz) due to the presence of the longitudinal resonator and the interaction between the same resonator and the transversal one. This fact has the consequence that a large number of poles is located near zero, as shown in Fig. 7.

The accuracy of transient broadband models of metamaterials is significantly dependent on such kind of poles as they determines the behavior in the low frequency range. The proposed MOR technique allows to select the most important low frequency poles thus preserving accuracy also below 200 MHz. Fig. 8 shows the selected poles providing excellent accuracy up to 50 GHz. Magnitude and phase of Y_{12} are shown in Fig. 9. The number of poles of the original model is 238 and that of the reduced one is 136. If only the criterion based on the magnitude of residues is used to select dominant poles, the number of poles decreases to 12 but the accuracy is lost below 100 MHz, as shown in Fig. 10

The importance of low frequency poles is then investigated looking at the magnitude of the corresponding residues for the same example VII-A. Fig. 11 shows the magnitude and phase spectra of

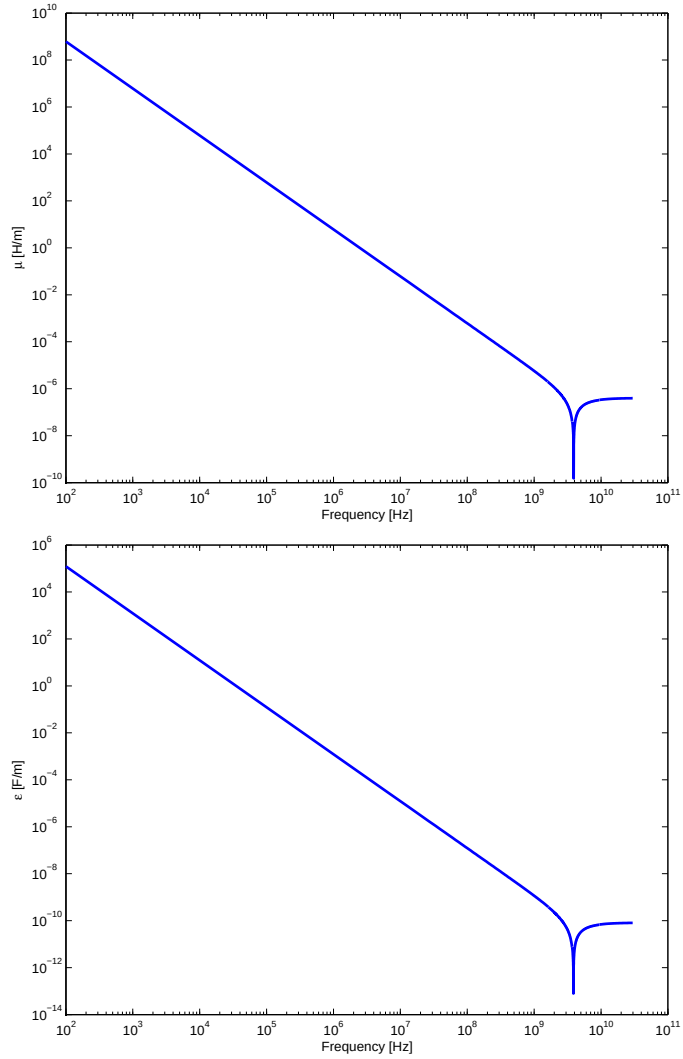

Fig. 4. Effective permeability (top) and permittivity (bottom) for example VII-A.

the Y_{12} function as obtained by considering the HTLN network (HTLN) and the reduced order model (MOR); if only the residue magnitude criterion is used in selecting poles, all the low frequency poles are excluded thus leading to loss of accuracy, as seen in Fig. 10. In this case a threshold $thresh = 1/100$ has been used. It is clearly recognized that neglecting poles with small residues in the low frequency range results into a significant error in modeling Y_{12} in the same frequency band.

The MMTL has been excited by a voltage source $v_s(t)$ whose time behavior is the second time derivative of a gaussian pulse; Fig. 12 shows the waveform along with the corresponding magnitude spectrum.

The output voltage is plotted in Fig. 13 as obtained by the HTLN model via IFFT by using all the poles (Reference) and by generating the reduced order macromodel and integrating the differential equation by means of the Gear-Shichman scheme (MOR-GE-SH) [48]. The two curves are practically overlapped. It is also worth to notice that causality is strictly preserved.

B. 2TDLM metamaterial

In the second test the 2TDLM metamaterial described in II-B has been considered. Such a medium is characterized by negative values of permeability and permittivity over a wide frequency range. Fig. 1 shows the real and imaginary part of the 2TDLM susceptibility with $\chi_\alpha = 1.0$, $\chi_\beta = 1.0 \times 10^{-5}$,

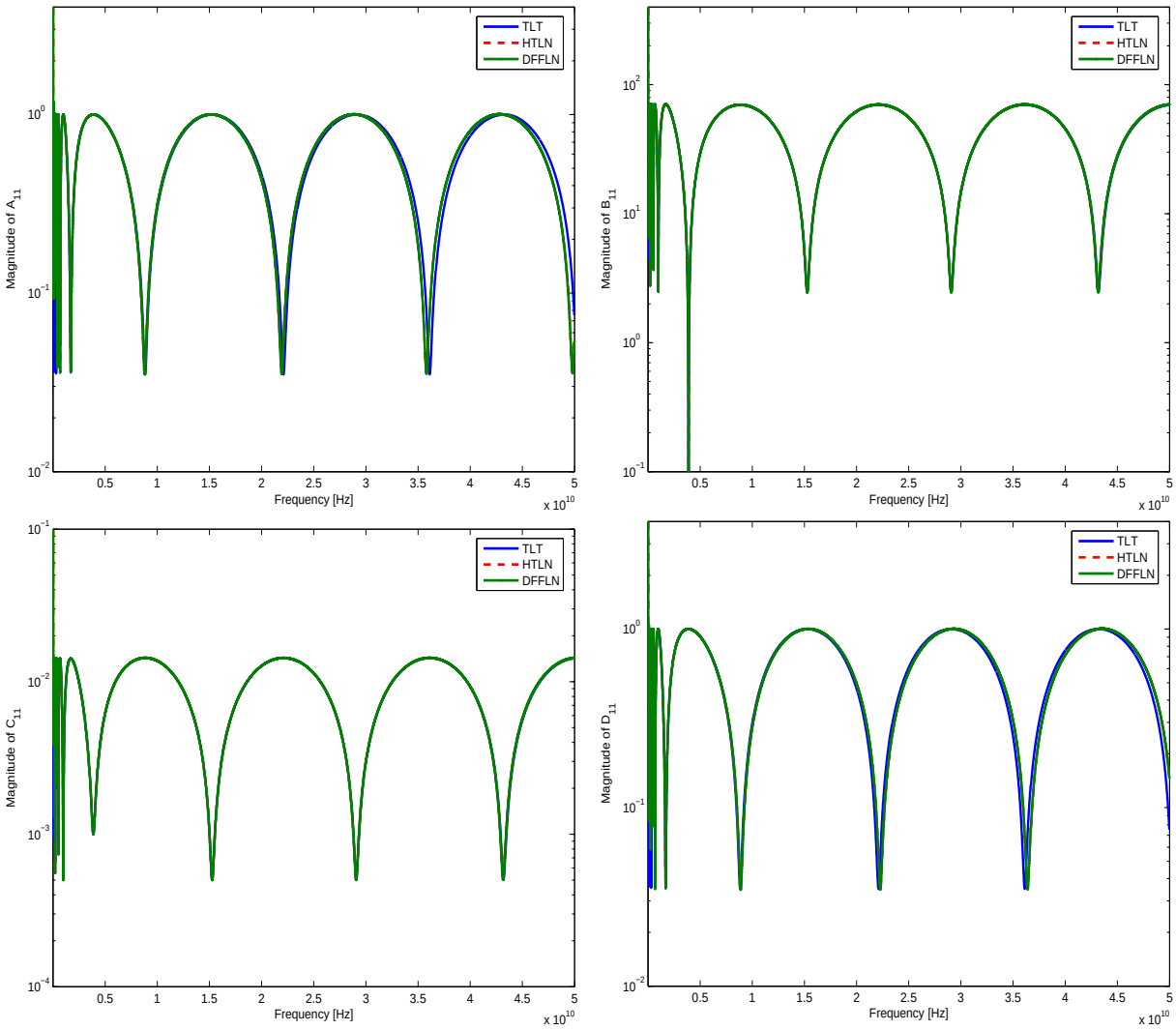

Fig. 5. Transmission coefficients ABCD for example VII-A. Upper left: A; upper right: B; lower right: C; lower right: D.

$\chi_\gamma = -0.5$, $\Gamma = 1.0 \times 10^{-1}\omega_0$ and $\omega_p = \omega_0 = 2\pi f_0$ for $f_0 = 1$ GHz. In [8] the propagation through a slab of such a metamaterial is computed by using a specialized 1-D FDTD code involving, besides electric and magnetic fields, polarization and magnetization fields as well to take into account the frequency dependence of equivalent $\mu(s)$ and $\varepsilon(s)$. The difficulty in carrying out a FDTD simulation involving dispersive media relies into the existence of many wave speeds in the system and, thus, Courant-Friedrichs-Levy (CFL) condition must be set carefully to achieve a stable algorithm. In the HTLN model proposed in this work stability is automatically guaranteed provided that a stable and passive model for the unit cell longitudinal impedance $Z_1(s)$ and transversal admittance $Y_2(s)$ are used. 2TDLM elementary cell is surely stable as it can be synthesized as a CRLH cell; as a consequence, the overall equivalent circuit is stable as well.

In order to reduce the effect of absorption near resonance, the parameters of the 2TDLM medium have been assumed as [8]: $\chi_\alpha = 1.0$, $\chi_\beta = 1.0 \times 10^{-5}$, $\chi_\gamma = -0.5$, $\Gamma = 1.0 \times 10^{-5}\omega_0$ and $\omega_p = \omega_0 = 2\pi f_0$ for $f_0 = 0.01$ GHz. As pointed out in [8], such parameter setting allows to preserve the shape of the single-cycle pulse having a peak frequency $f_{00} = 1$ GHz which should travel without distortion at the speed 2 c_0 through the slab.

A 20 cm long MMTL has been considered. The MOR technique has been applied leading to a reduced set of poles well describing the behavior of the MMTL in the frequency range 0-30 GHz. The

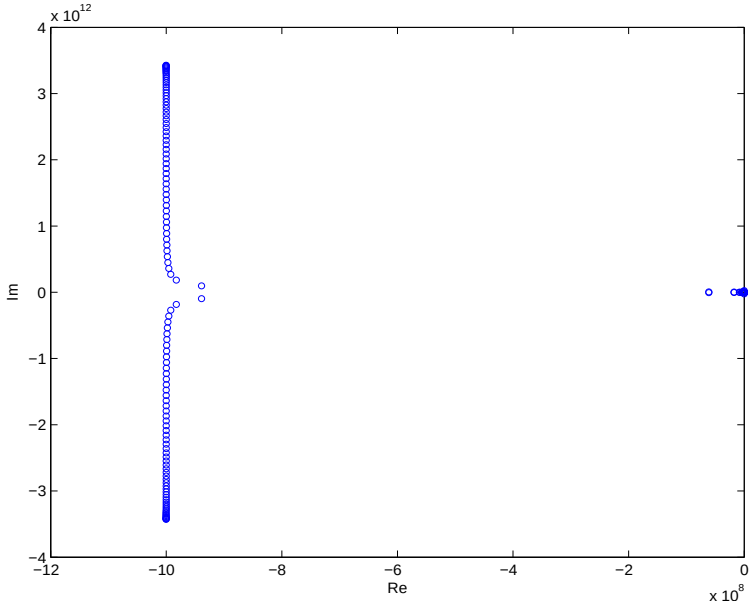

Fig. 6. Location of poles in the complex plane for example VII-A.

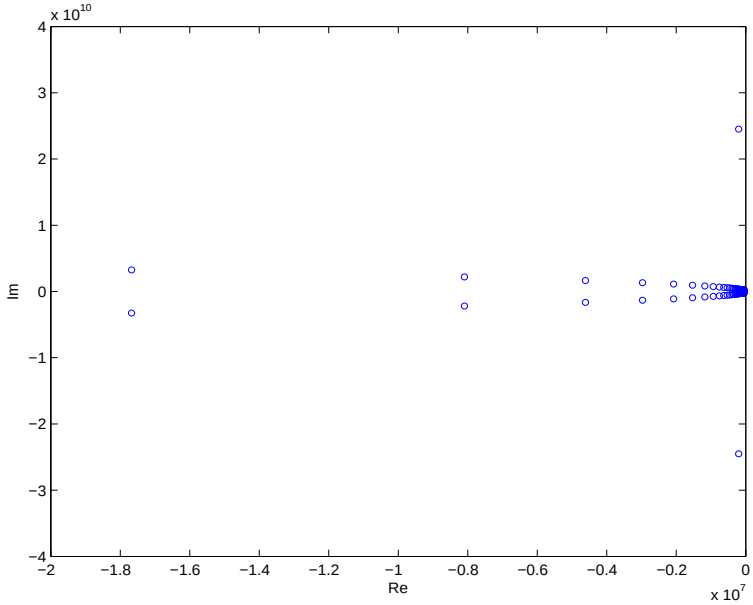

Fig. 7. Zoom of poles around zero for example VII-A.

initial set of 357 poles has been reduced to only 53. Fig. 15 shows the magnitude spectra of Y_{11} and Y_{21} as evaluated by the transmission line theory (TLT) and the proposed reduced order model (MOR); as seen, a very good accuracy is achieved over the entire frequency range. In order to check the accuracy of the reduced order model the Feature Selective Validation procedure has been applied. The Feature Selective Validation (FSV) techniques aims to perform the comparison of different datasets by mimic the behavior of a group of experienced engineers when they perform such a comparison by means of a visual approach [49]-[51]. The FSV method is based on the decomposition of the original data into two parts: amplitude (trend/envelope) data and feature data. The former component accounts for the slowly varying data across the data set and the latter accounts for the sharp peaks and troughs often found in CEM data. The numerical figures of merit obtained as output from the FSV procedure

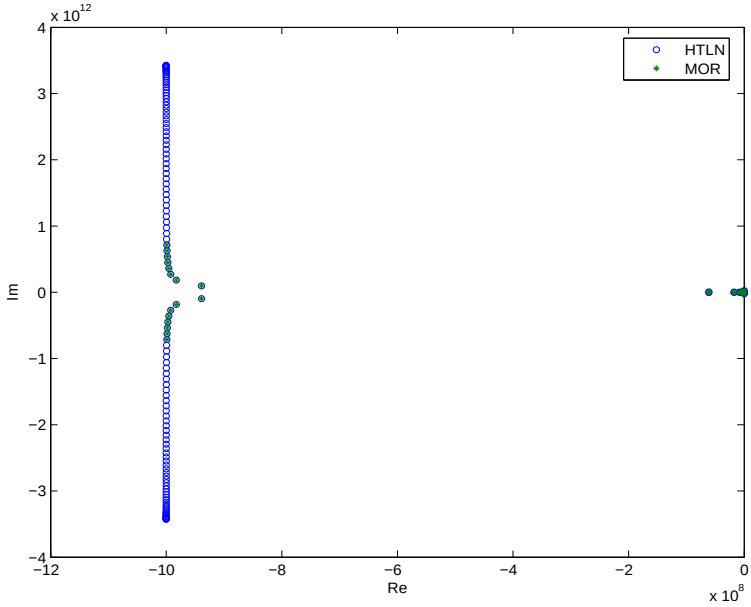

Fig. 8. Model order reduction for example VII-A: selected poles in the half left complex plane.

can be converted in a natural language descriptor (excellent, very good, good, fair, poor, very poor comparison). The essential meaning of the FSV figures of merit are: ADM (Amplitude Difference Measure), FDM (Feature Difference Measure) and GDM (Global Difference Measure). ADM and FDM can be combined by using a Grade-Spread chart which gives a numerical value to the Grade by counting how many categories are required (starting from Excellent) for the cumulative total of the histogram to exceed a given value. A numerical value is given to the Spread by counting how many adjacent categories (starting from the largest) are required to cumulatively exceed a given value.

The models obtained considering all the poles and only the dominant ones have been compared over the frequency range 0-30 GHz. Fig. 16 shows the FSV comparison of the magnitude of Y_{12} matrix entry. As seen, all the figures of merit confirm that the reduced order model perfectly captures the physics of the system and provides a very good approximation over the entire frequency band 0-30 GHz.

A single-cycle pulse for the source of unit amplitude is used to excite the material:

$$f(t) = \begin{cases} \sqrt{7}\,(7/6)^3 \left(\frac{t-T_p/2}{T_p/2}\right)\left[1-\left(\frac{t-T_p/2}{T_p/2}\right)^2\right]^3 & \text{for } 0 \le t \le T_p \\ 0 & \text{for } t > T_p \end{cases} \tag{45}$$

where T_p is the length of time the pulse has a non-zero value; in the simulation it has been assumed $T_p = 1$ ns.

Fig. 17 shows the single cycle pulse used as source of the MMTL in example VII-B along with its frequency magnitude spectrum.

Fig. 18 shows the voltages of the 2DTLM transmission line as obtained by using both the transmission line theory via inverse Fourier Transform (TLT-IFFT) and the proposed macromodel after the pole pruning has been performed (MOR-Macromodel).

It is worth of notice that, as expected, the input pulse propagates through the MMTL, at speed 2 c_0, with almost no attenuation. Also, it is to be observed that the proposed model strictly preserves causality.

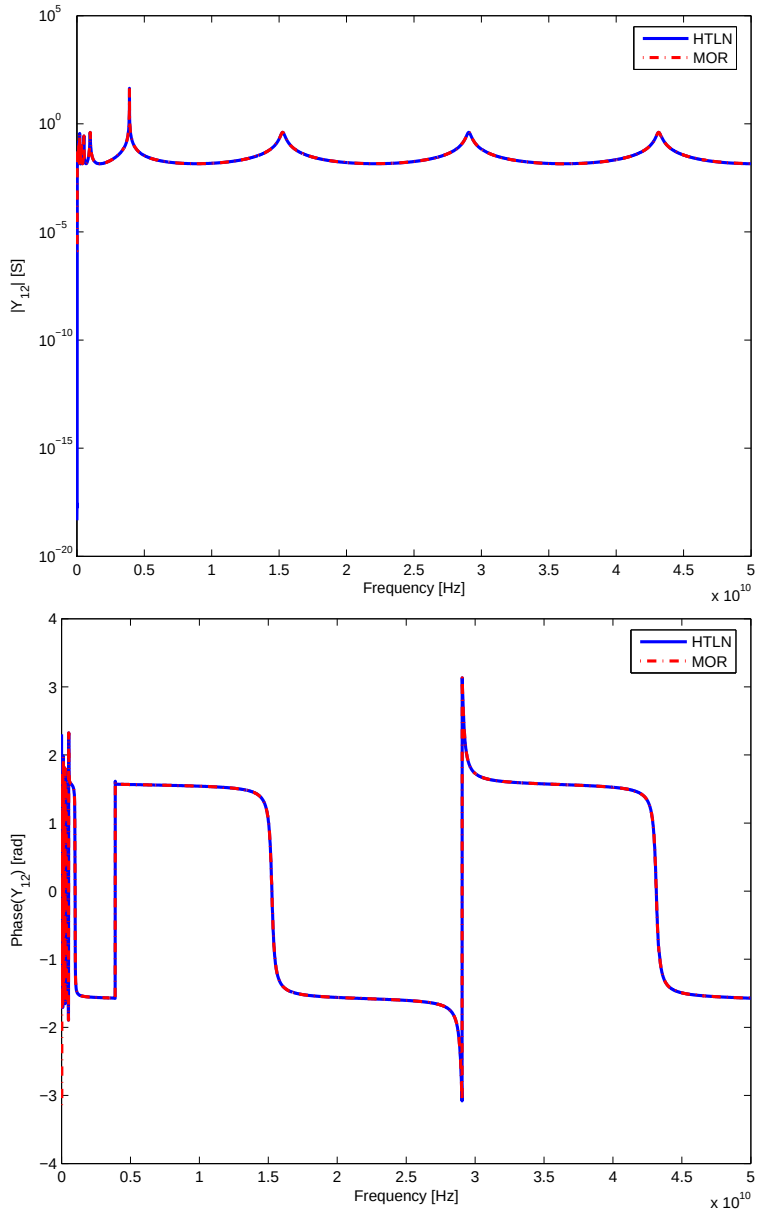

Fig. 9. Model order reduction for example VII-A. Top: magnitude of Y_{12}, bottom: phase of Y_{12}.

C. Parameterized CRLH-TL

As last example a macromodel has been generated for a MMTL for several different values of L_L. Fig. 19 shows the location of poles in the left half complex plane for increasing values of L_L and $L_R = 4.7$ nH, $C_R = 0.1$ pF, $C_L = 9.6$ pF, $R = 1$ mΩ, $G = 1$ mS, $l = 120$ mils.
It is clearly seen that all the poles have a strict negative real part, thus ensuring the stability of the macromodel, and that, increasing the value of L_L, results into a reduction of the imaginary part of complex poles.
The transmission line has been modeled as a 20-th order half-T ladder network, with 78 poles; the reduced order model has been generated to be accurate within the 0-30 GHz range; only four poles have been selected as dominant ones. Thus, extremely simplified state-space models are generated, at a reduced cost, for different values of L_L. Fig. 20 shows the output voltage of the CRLH-TL excited by a normalized second order derivative of a gaussian pulse.

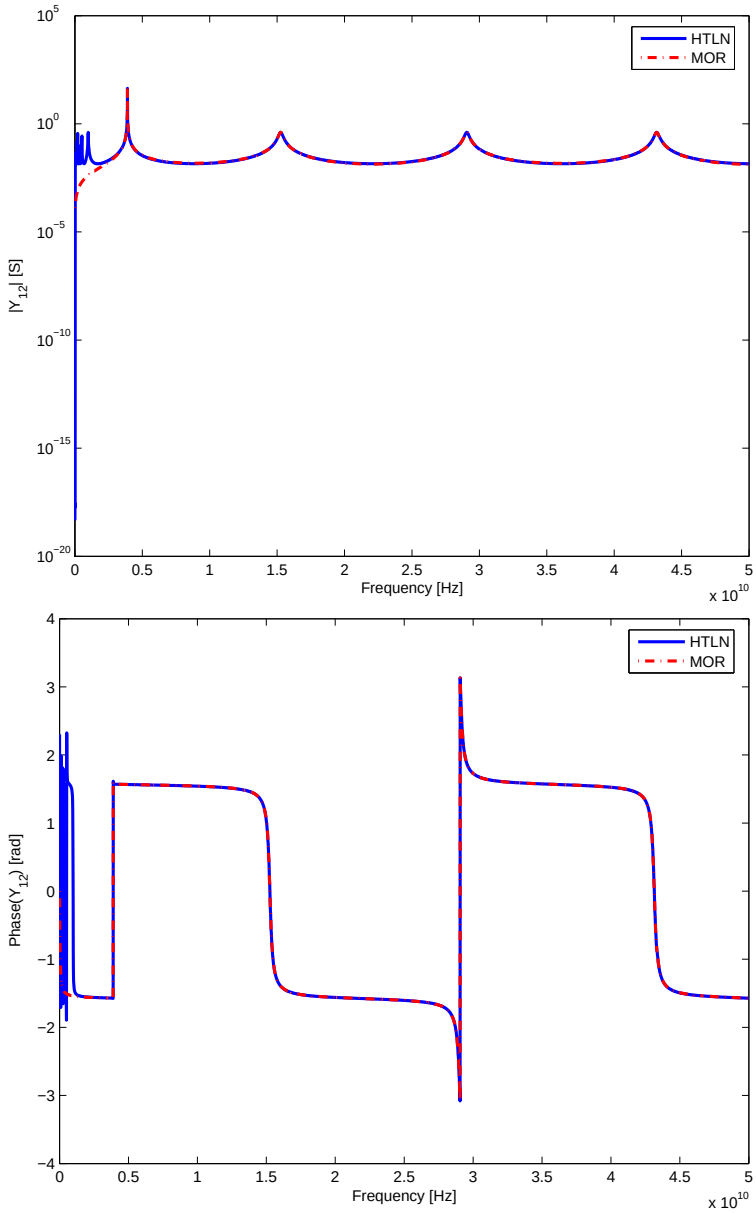

Fig. 10. Not accurate model order reduction in the low frequency range for example VII-A. Top: magnitude of Y_{12}, bottom: phase of Y_{12}.

VIII. Conclusions

A general methodology for the transient analysis of MMTLs has been presented. A rational approximation of the metamaterial transmission line is obtained by extracting the poles of the Y matrix representation of the half-T ladder network describing the MMTL; pole pruning allows the generation of a reduced order macromodel which has been used for carrying out accurate transient analysis of MMTLs. The proposed methodology can be applied to any type of metamaterial and/or lossy and dispersive medium being based on a polynomial closed-form representation of half-T ladder network which is totally independent on the nature of materials; moreover it can be used as a building block for modeling dispersive materials in the framework of TLM method. The robustness and accuracy of the method has been confirmed by the numerical results; in particular typical metamaterial phenomena such as superluminal speeds of propagation over a large band of frequencies and well separated stop/pass bands have been successfully modeled.

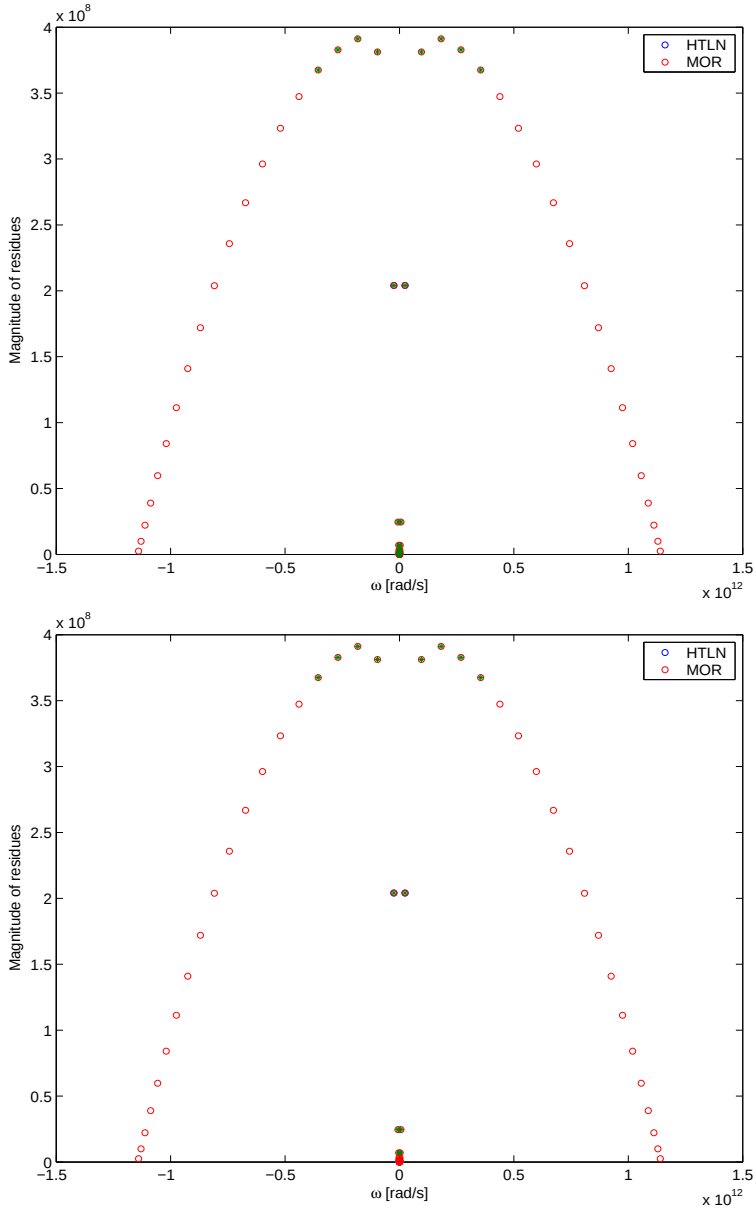

Fig. 11. Magnitude of residues for example VII-A. Top: including all the low frequency poles; bottom: excluding low frequency poles with residues below the fixed threshold.

References

[1] V. G. Veselago. The electrodynamics of substances with simultaneously negative values of ε and μ (in Russian). *Usp. Fiz. Nauk.*, 92:517–526, 1967.

[2] V. G. Veselago. The electrodynamics of substances with simultaneously negative values of ε and μ. *Sov. Phys. Usp.*, 47:509–514, Jan.-Feb., 1968.

[3] J. B. Pendry, A. J. Holden, D. J. Robins and W. J. Stewart. Magnetism from conductors and enhanced nonlinear phenomena. *IEEE Transactions on Microwave Theory and Techniques*, 47(11):2075–2084, November 1999.

[4] D. R. Smith, D. C. Vier, W. J. Padilla,, S. C. Nemat-Nasser and S. Schultz. Loop-wire for investigating plasmons at microwave frequencies. *Appl. Phys. Lett.*, 75(10):1425–1427, September 1999.

[5] D. R. Smith, W. J. Padilla, D. C. Vier, S. C. Nemat-Nasser and S. Schultz. Composite medium with simultaneously negative permittivity and permeability. *Phys. Rev. Lett.*, 84:4184–4187, May 2000.

[6] G. V. Eleftheriades, O. Siddiqui and A. K. Iyer. Transmission Line Models for negative Refractive Index Media and Associated Implementations Without Excess Resonators. *IEEE Microwave and Wireless Components Letters*, 13(2):51–53, February 2003.

[7] C. Caloz and T. Itoh. Transmission Line Approach of Left-Handed (LH) Materials and Microstrip Implementation of an Artificial LH Transmission Line. *IEEE Transactions on Antennas and Propagation*, 52(5):1159–1166, May 2004.

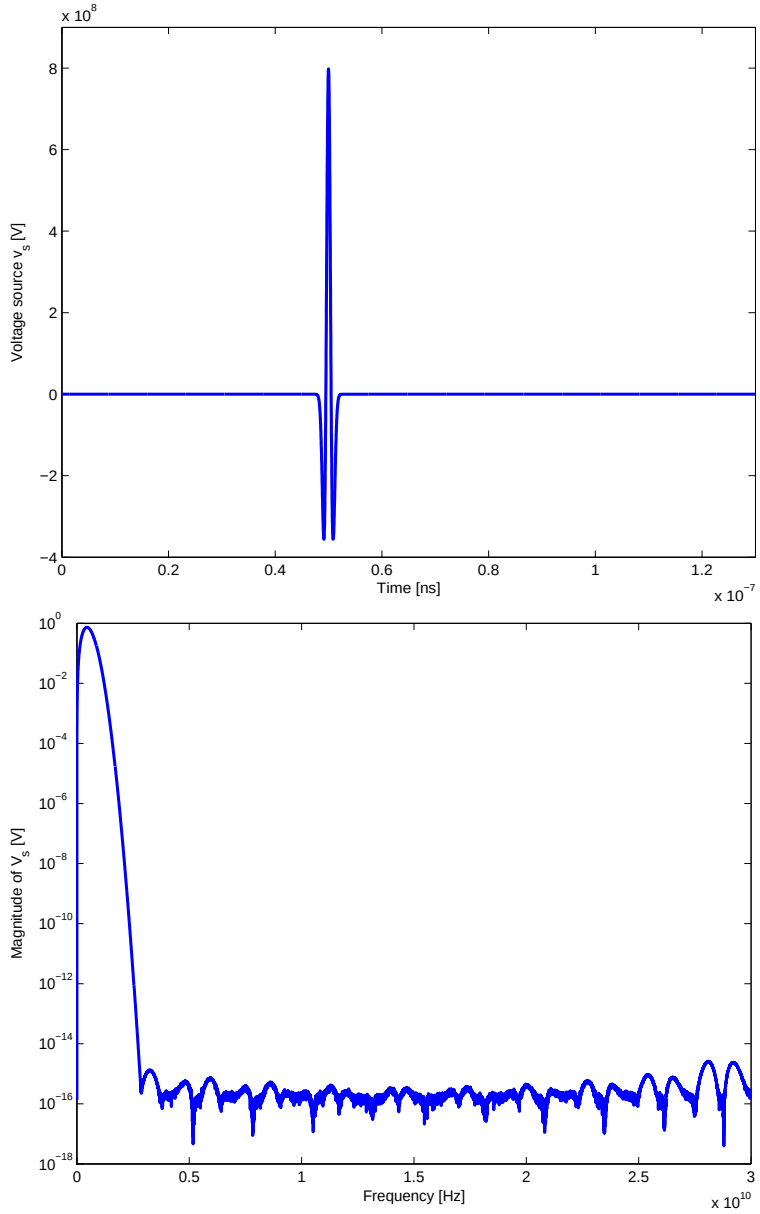

Fig. 12. CRLH-TL excitation (example VII-A). Top: time domain waveform v_s; bottom: magnitude spectrum of V_s.

[8] R. W. Ziolkowski. Superluminal transmission of information through an electromangetic metamaterial. *Phys. Rev. E*, 63, 2001.

[9] M. W. Feise, J. B. Schneider and P. J. Bevelacqua. Finite-Difference and Pseudospectral Time-Domain Methods Applied to Backward-Wave Metamaterials. *IEEE Transactions on Antennas and Propagation*, 52(11):2955–2962, November 2004.

[10] Q. H. Liu. The PSTD algorithm: a time-domain method requiring only two cells per wavelength. *Microwave and Optical Technology Letters*, 15(3):158–165, June 1997.

[11] A. Lai, C. Caloz and T. Itoh. Composite Right/Left-Handed Transmission Line Metamaterals. *IEEE Antenna and Propagation Magazine*, pages 34–50, September 2004.

[12] A. Grbic and G. V. Eleftheriades. Negative Refraction, Growing Evanescent Waves and Sub-Diffraction Imaging in Loaded Transmission-Line Metamaterials. *IEEE Transactions on Antennas and Propagation*, 51(12):2297–2305, December 2003.

[13] A. Sanada, C. Caloz and T. Itoh. Characteristics of the Composite Right/Left-Handed Transmission Lines. *IEEE Microwave and Wireless Components Letters*, 14(2):68–70, November 2004.

[14] Y. Horii, C. Caloz, T. Itoh. Super-compact Multilayered Left-Handed Transmission Line and Diplexer Application. *IEEE Transactions on Microwave Theory and Techniques*, 53(4):1527–1534, April 2005.

[15] P. P. So and W. J. R. Hoefer. Time Domain TLM Modeling of Metamaterials with Negative Refractive Index. In *2004 IEEE MTT-S Int. Microwave Symp. Dig.*, pages 1779–1782, Jun 2004.

[16] P. P. So, H. Du and W. J. R. Hoefer. Modeling of metamaterials with negative Refractive Index uisng 2-D shunt and 3-D SCN TLM networks. *IEEE Transactions on Microwave Theory and Techniques*, 53(4):1496–1505, April 2005.

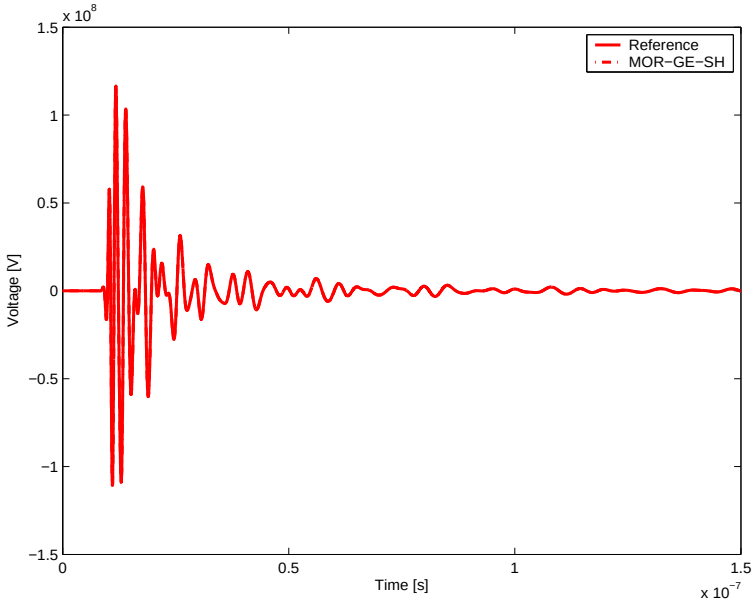

Fig. 13. Output voltage (example VII-A).

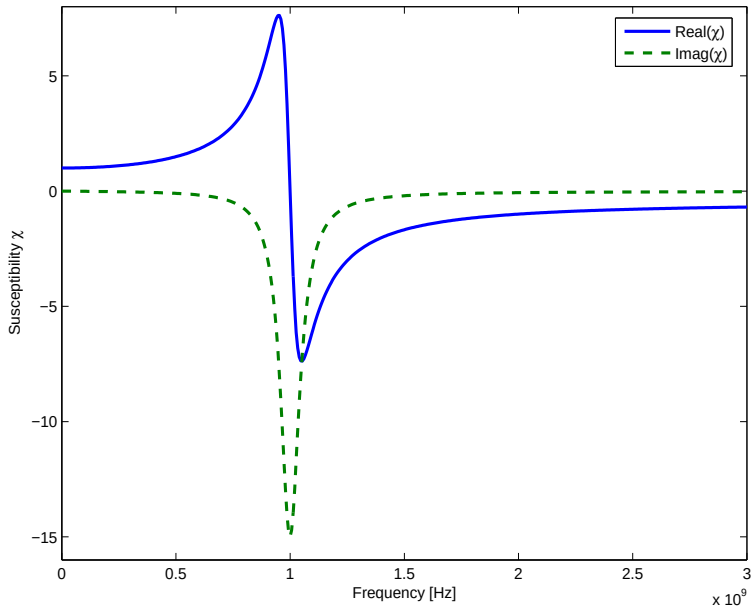

Fig. 14. Real and imaginary part of the 2TDLM susceptibility of example VII-B with $\chi_\alpha = 1.0$, $\chi_\beta = 1.0 \times 10^{-5}$, $\chi_\gamma = -0.5$, $\Gamma = 1.0 \times 10^{-5}\omega_0$ and $\omega_p = \omega_0 = 2\pi f_0$ for $f_0 = 1$ GHz.

[17] A. Rennings, S. Otto, C. Caloz, A. Lauer, W. Bilgic and P. Waldow. Composite right/left-handed extended equivalent circuit (CRLH-EEC)FDTD: Stability and disperion analysis with examples. *International Journal Numerical Modeling*, 19:141–172, 2006.

[18] W. J. R. Hoefer. *The transmission line matrix (TLM) method.* in Numerical Techniques for Microwave and Millimeter Wave Passive Structures, (T. Itoh, ed), Wiley, N.Y., 1989.

[19] W. J. R. Hoefer. Transmission line matrix (TLM) models of electromagnetic fields in space and time. In *Proceedings International Zurich Symposium on EMC*, volume 11, Zürich, Switzerland, February 1997.

[20] C. Christopoulos. *An introduction to the Transmission-Line Modelling (TLM method).* IEEE Press, New York, 1992.

[21] J. Paul, C. Christopoulos and D. W. P. Thomas. Generalzed Material Models in TLM - Part I: Materials with Frequency-Dependent Properties. *IEEE Transactions on Antennas and Propagation*, 47(10):1528–1534, October 1999.

[22] G. Antonini, A. Orlandi. Ultra Wide Band Plane Waves Propagation Through Lossy and Dispersive Media. In *EMC Europe Workshop 2005: EMC of Wireless Systems*, Roma, Italy, September 2005.

[23] R. Achar, M. Nakhla. Simulation of High-Speed Interconnects. *Proceedings of the IEEE*, 89(5):693–728, May 2001.

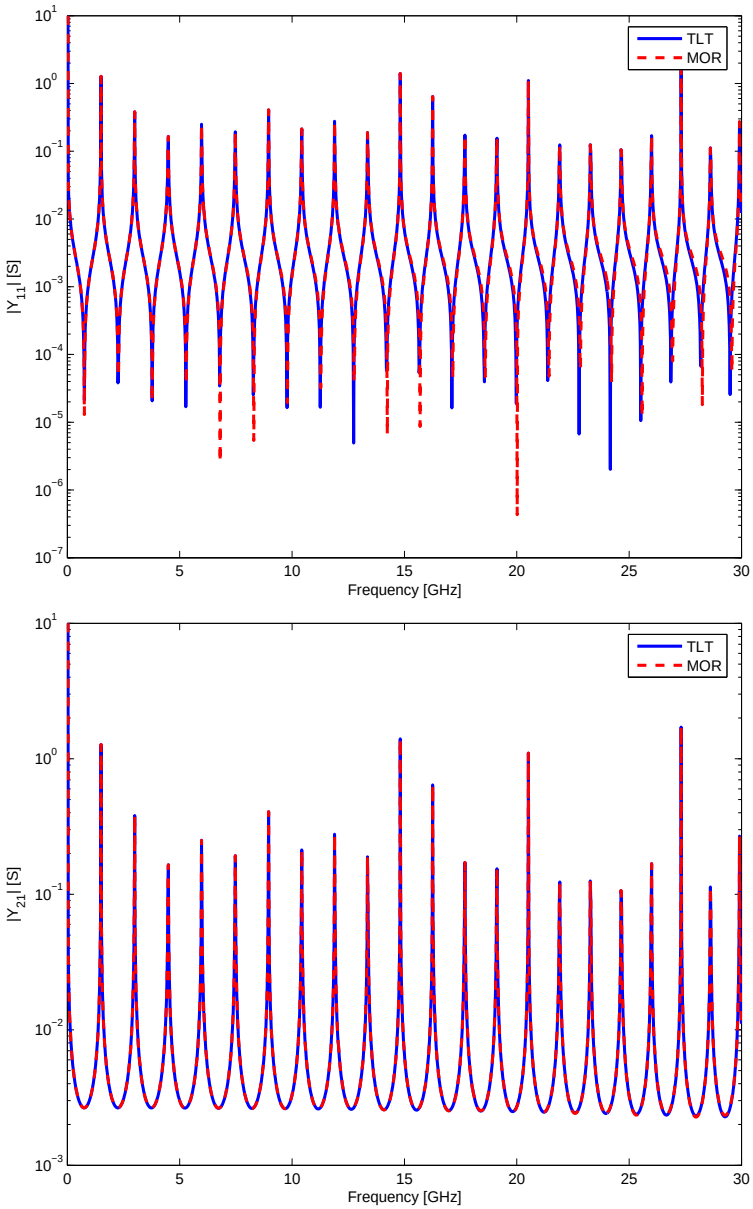

Fig. 15. Comparison of $\boldsymbol{Y}$ matrix entries for example VII-B. Top: Y_{11} magnitude spectrum; bottom: Y_{21} magnitude spectrum.

[24] M. S. Nakhla R. Achar A. Dounavis, X. Li. Passive Closed-Form Transmission-Line Model for General-Purpose Circuit Simulators. *IEEE Transactions on Microwave Theory and Techniques*, 47(12):2450–2459, December 1999.

[25] A. Dounavis, R. Achar, M. Nakhla. Efficient Passive Circuit Models for Distributed Networks with Frequency-Dependent Parameters. *IEEE Transactions on Advanced Packaging*, 23(3):382–392, August 2000.

[26] A. Dounavis, R. Achar, M. Nakhla. A General Class of Passive Macromodels for Lossy Multiconductor Transmission Lines. *IEEE Transactions on Microwave Theory and Techniques*, 49(10):1686–1696, October 2001.

[27] I. M. Elfadel, H-M. Huang, A. E. Ruehli, A. Dounavis, M. S. Nakhla. A Comparative Study of Two Transient Analysis Algorithms for Lossy Transmission Lines With Frequency-Dependent Data. *IEEE Transactions on Advanced Packaging*, 25(2), May 2002.

[28] G. Antonini, G. Ferri. A New Approach for Closed-Form Transient Analysis of Multiconductor Transmission Lines. *IEEE Transactions on Electromagnetic Compatibility*, 46(4):529–543, November 2004.

[29] M. Faccio, G. Ferri, A. D'Amico. The DFF and DFFz Triangles and Their Mathematical Properties. *Applications of Fibonacci Numbers, G. E. Bergum et al.,(eds)*, 5:199–206, 1990.

[30] M. Faccio, G. Ferri, A. D'Amico. A New Fast Method for Ladder Networks Characterization. *IEEE Transactions on Circuits and Systems, I*, 38(11):1377–1382, September 1991.

[31] G. Ferri, M. Faccio, A. D'Amico. Fibonacci Numbers and Ladder Network Impedance. *Fibonacci Quarterly*, 30:62–67, February 1992.

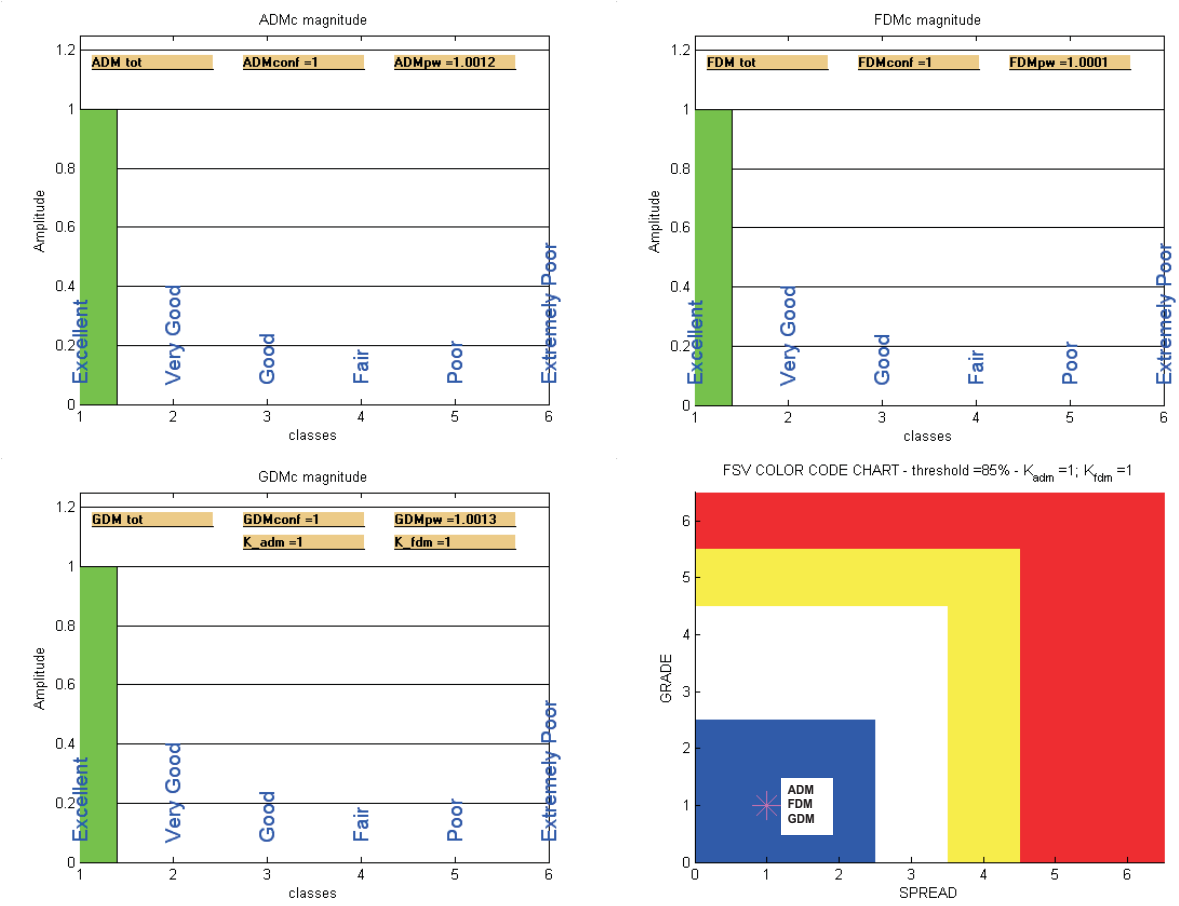

Fig. 16. ADMc, FDMc GDMc confidence histograms and Grade-Spread chart.

[32] G. Antonini. A New Methodology for the Transient Analysis of Lossy and Dispersive Multiconductor Transmission Lines. *IEEE Transactions on Microwave Theory and Techniques*, 52(9):2227–2239, September 2004.

[33] S. Ramo, J. R. Whinnery and T. Van Duzer. *Fields and Waves in Communication Electronics*. John Wiley and Sons, New York, 1994.

[34] A. Alù, N. Engheta. Pairing an epsilon-negative slab with a mu-megative slab: resonance, tunneling and tranparency. *IEEE Transactions on Antennas and Propagation*, 51(10):2558–2571, October 2003.

[35] C. R. Paul. *Analysis of Multiconductor Transmission Lines*. John Wiley & Sons, New York, NY, 1992.

[36] J. Brandão Faria. *Multiconductor Transmission-Line Structures: Modal Analysis Technique*. John Wiley & Sons, New York, NY, 1993.

[37] B. Gustavsen and A. Semlyen. Rational Approximation of Frequency Domain Responses by Vector Fitting. *IEEE Transactions on Power Apparatus and Systems*, 14(3):1052–1061, July 1999.

[38] G. Strang, T. Nguyen. *Wavelets and Filter Banks*. Wellesley, Cambridge Press, MA, 1997.

[39] G. Antonini, G. Ferri. Compact Transmission Lines Representation. *IEE Proceedings-Science, Measurement and Technology*, 151(3):211–217, May 2004.

[40] L. T. Pillage and R. A. Rohrer. Asymptotic Waveform Evaluation for Timing Analysis. *IEEE Transactions on Computer-Aided Design*, 9(4):352–366, 1990.

[41] E. Chiprout, M.S. Nakhla. *Asymptotic Waveform Evaluation*. KLUWER, 1994.

[42] K. Gallivan, E. Grimme, P. Van Dooren. Asymptotic Waveform Evaluation Via a Lanczos Method. *Applied Math.*, 7(5):75–80, September 1994.

[43] L. Pillegi, R. Rohrer, C. Visweswariah. *Electronic Circuits and System Simulation Methods*. McGraw-Hill Book Company, 1995.

[44] T. Kailath. *Linear Systems*. Prentice Hall, Englewood Cliffs, NJ, 1980.

[45] C. T. Chen. *Linear System Theory and Design*. Holt, Rinehart, Winston, New York, 1984.

[46] A. Ruberti, S. Monaco. *Teoria dei Sistemi*. Pitagora Editrice Bologna, 1998.

[47] R. Neumayer, A. Steltzer, F. Haslinger, R. Weigel. On the Synthesis of Equivalent-Circuit Models for Multiports Characterized by Frequency-Dependent Parameters. *IEEE Transactions on Microwave Theory and Techniques*, 50(12):2789–2796, December 2002.

[48] H. Shichman. Integration system of a nonlinear network analysis program. *IEEE Transactions on Circuits and Systems*, 17:378–386, August 1970.

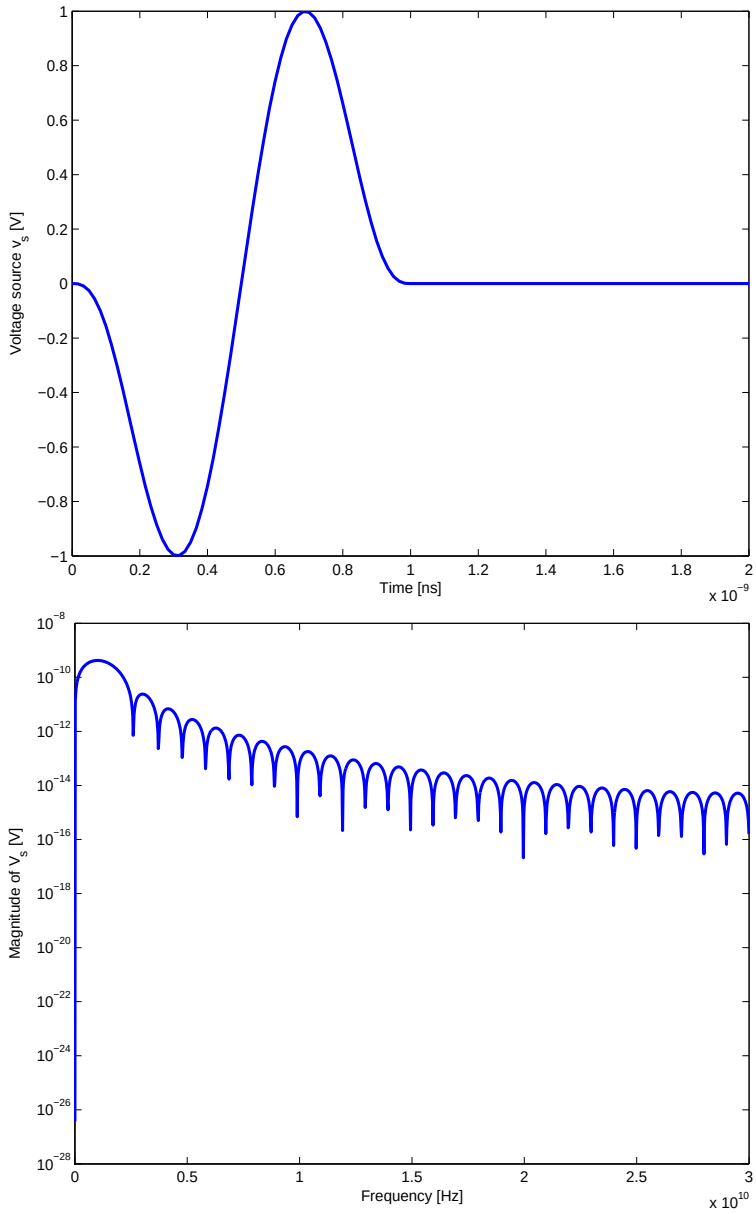

Fig. 17. Single cycle pulse excitation for example VII-B. Top: time domain waveform; bottom: frequency magnitude spectrum.

[49] A. Duffy, A. Martin, G. Antonini, A. Orlandi, C. Ritota. The Feature Selective Validation (FSV) Method. In *Proc. of the IEEE Int. Symp. on Electromagnetic Compatibility*, Chicago, IL, USA, August 2005.

[50] A. Duffy, A. Martin, A. Orlandi, G. Antonini, T. M. Benson, M. Woolfson. Feature Selective Validation (FSV) for validation of Computational Electromagnetics (CEM). Part I - The FSV Method. *IEEE Transactions on Electromagnetic Compatibility*, 48(2), August 2006.

[51] A. Duffy, A. Martin, A. Orlandi, G. Antonini, T. M. Benson, M. Woolfson. Feature Selective Validation (FSV) for validation of Computational Electromagnetics (CEM). Part II - Numerical Verification. *IEEE Transactions on Electromagnetic Compatibility*, 48(2), August 2006.

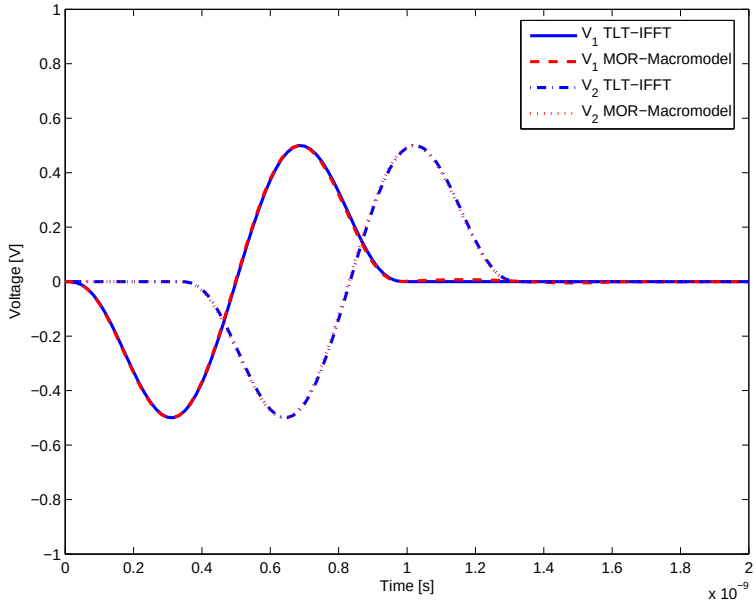

Fig. 18. Comparison of voltages at the input and output ports of a 2TDLM transmission line for example VII-B.

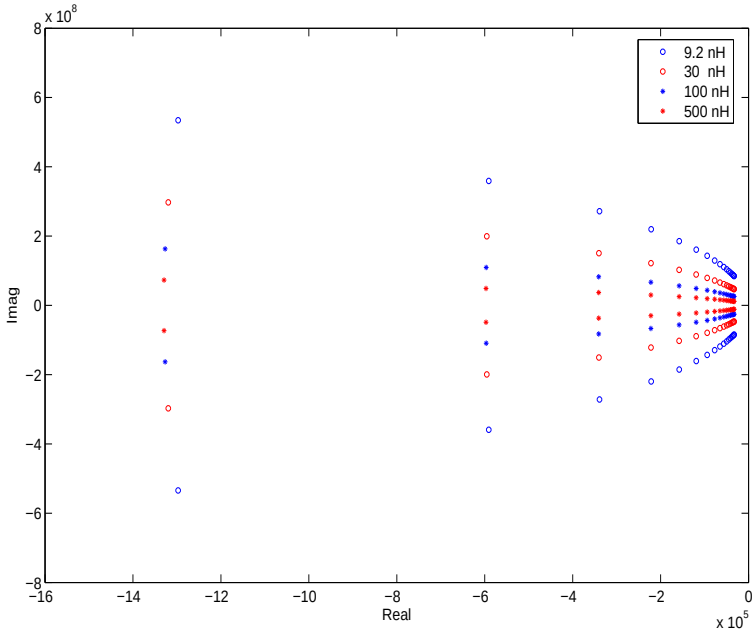

Fig. 19. Poles location in the complex plane for increasing values of L_L (example VII-C).

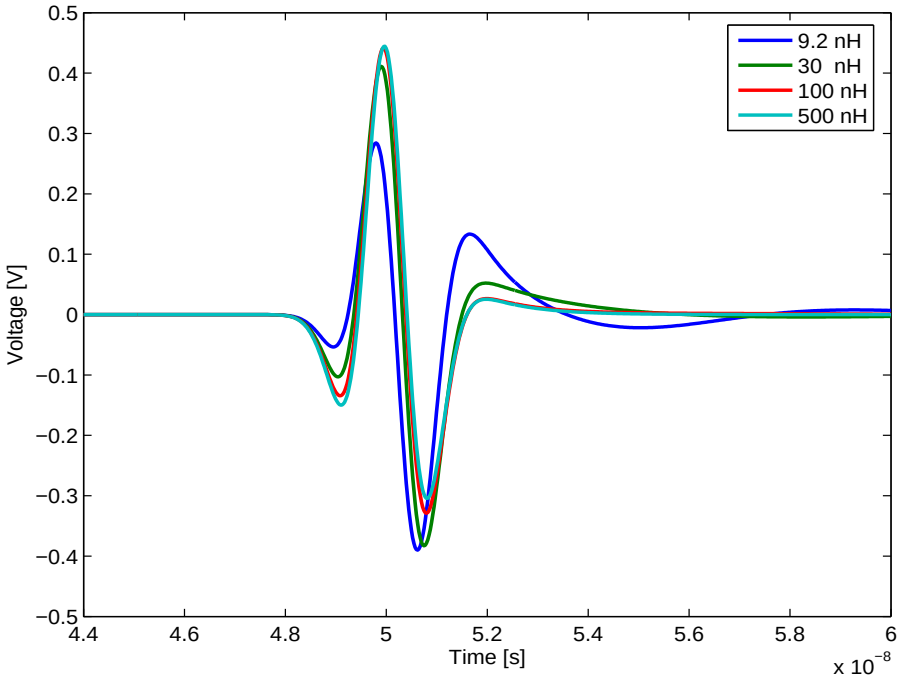

Fig. 20. Output voltage of the CRLH-TL for different values of L_L (example VII-C).